Comparative studies on field-induced stretching behavior of single-walled and multiwalled carbon nanotube clusters

Weiwei Tie,[1,4] Surjya Sarathi Bhattacharyya,[1,3] Hye Ryung Park,[1] Joong Hee Lee,[1] Sang Won Lee,[2] Tae Hoon Lee,[2] Young Hee Lee,[2,*] and Seung Hee Lee[1,†]

[1]*Applied Materials Institute for BIN Convergence, Department of BIN Fusion Technology and Department of Polymer Nano-Science and Technology, Chonbuk National University, Jeonju, Jeonbuk 561-756, Korea*

[2]*IBS Center for Integrated Nanostructure Physics, Institute for Basic Science, and Department of Energy Science and Department of Physics, Sungkyunkwan University, Suwon 440-746, Korea*

[3]*Asutosh College, 92, Shyamaprasad Mukherjee Road, Kolkata, 700 026, West Bengal, India*

[4]*Key Laboratory of Micro-Nano Materials for Energy Storage and Conversion of Henan Province, Institute of Surface Micro and Nano Materials, School of Advanced Materials and Energy, Xuchang University, Xuchang, Henan, 461000, China*

(Received 4 March 2014; published 24 July 2014)

We demonstrate distinct entanglement of single-walled carbon nanotube (SWCNT) and multiwalled carbon nanotube (MWCNT) clusters in nematic liquid crystal medium using scanning electron microscopy technique and the entanglement influence on electric field-induced stretching phenomena of the said clusters in the same medium under optical microscopy investigation. The observed stretching threshold field for MWCNT clusters is found to be higher than the SWCNT counterpart caused by the interplay between attractive field-induced dipolar interaction of intercarbon nanotube (CNT) bundles and the distinct degree of entanglement of neighboring CNT bundles. Subsequently observed different tensile elasticity modulus results for different CNT kinds also confirm different CNT bundle entanglement and attractive dipolar interaction between adjacent CNT bundles in CNT clusters are responsible for distinct stretching threshold field behavior.

DOI: 10.1103/PhysRevE.90.012508 PACS number(s): 61.30.−v, 61.48.De, 62.20.de, 31.30.jn

I. INTRODUCTION

The highly anisotropic structure and excellent elastic properties have stimulated research on carbon nanotubes (CNTs) [1–5], which cover an impressively diverse range of applications including optical polarizers; field emitters; field-effect transistors; actuators; ultrasensitive mechanical, physical, and chemical sensors and biosensors; alignment layers; and transparent conducting film for liquid crystal display [6–14]. Nevertheless, the cluster forming tendency of individual CNTs due to strong van der Waals interaction between them has greatly nullified their unidirectional anisotropic properties, which further limits their large-scale applications. In order to obtain uniform CNT alignment, studies using groove surface and orientational ordering of liquid crystals are performed [15,16] but the volume concentration of aligned CNTs in the host material is limited.

Fortunately, electric field-induced stretching behavior of CNT clusters [17–20] has shown promising potential for macroscopic alignment of CNT clusters along a predetermined direction. In the presence of electric field, the randomly aligned CNTs in clusters are aligned along the field direction to minimize the dipolar energy. With further increasing field, the CNT clusters could be stretched along the field direction above the threshold field against van der Waals force between individual CNTs. More importantly, the electric field-induced stretched CNT clusters within the elastic limit show excellent reliability in reversible electric field-induced stretching behavior as an elastic body, and possess anisotropic absorption of visible light [18,19]. Such selective absorption properties have been utilized for realizing an electrically tunable carbon nanotube polarizer [19], which will play a vital role in fabrication of various electro-optic and photonic devices.

Single-walled carbon nanotubes (SWCNTs) are cylinders of single-layer graphene sheet composed of hexagonal packing of carbon atoms, whose diameters are typically less than 2 nm. Individual SWCNTs are floppy and can be easily bundled together. On the other hand, multiwalled carbon nanotubes (MWCNTs) are concentric cylinders of multishell graphene sheets. The outer MWCNT diameter expands typically from 3 to 100 nm [21]. These are more rigid than SWCNTs, although smaller-diameter MWCNTs have a similar tendency of bundling. This structural difference strongly affects the CNT dispersion and mechanical properties [22–24]. Although we have demonstrated the CNT cluster size-dependent stretching threshold [17,18] in our previous investigation, it does not point out the significant difference of stretching threshold behavior of self-assembled CNT clusters due to difference in respective structures from SWCNT to MWCNT cases. Therefore, in this study we perform an investigation on in-plane electric field-induced elastic stretching of SWCNT and MWCNT clusters. Comparison of the stretching threshold field and tensile elasticity modulus between MWCNT and SWCNT clusters is extensively discussed.

II. EXPERIMENTS

The SWCNT and thin MWCNT powders are purchased from Unidym (USA) and Hanhwa nanotechnology (Korea). The MWCNTs have an outer diameter of 3–6 nm and lengths of a few tens of micrometers. The SWCNTs have a diameter of 0.8–1.2 nm with lengths from one to tens of micrometers. These CNTs are cut by the following procedure [19]. The

*leeyoung@skku.edu
†lsh1@chonbuk.ac.kr

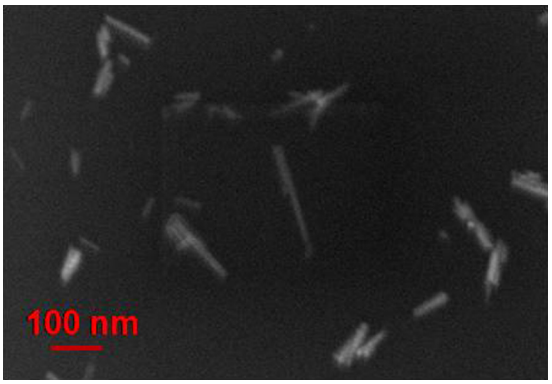

FIG. 1. (Color online) SEM image of dispersed SWCNTs in NLC medium.

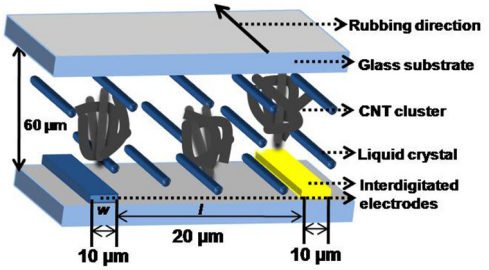

FIG. 2. (Color online) Illustration of test cell driven by in-plane field.

respective SWCNT and thin MWCNT powders of 100 mg are stirred in 1M sucrose solution for 1 h. The sucrose-mediated SWCNTs and thin MWCNTs are ground in a mortar for 30 min and 1 h, respectively. The ground SWCNTs and thin MWCNTs of 5 mg are dispersed in 30 ml ethanol of by sonication for 15 min. The ground MWCNTs have a length distribution of 150–550 nm with an average value of ∼290 nm [19] while the ground SWCNTs have a length distribution of 80–200 nm with an average value of ∼100 nm (Fig. 1). The length difference between SWCNT and MWCNT after grinding is attributed to the stronger mechanical strength of MWCNTs. The dispersions with a CNT concentration of 0.167 g/ml are mixed with a negative dielectric anisotropic nematic liquid crystal (NLC), MJ98468, fabricated by Merck-Japan. The NLC material used for the present investigation possesses dielectric anisotropy $\Delta\varepsilon = -4$, rotational viscosity $\gamma = 153$ mPa s, and clearing temperature of 75 °C. Special care is taken to remove ethanol solvent using a solvent evaporator kept at 70 °C. The homogeneous CNT-NLC mixtures for either kind with a CNT concentration of 10^{-3} wt % are thus finally achieved following identical experimental methods as described in our previous work [25].

The length of ground SWCNTs and the cluster structures of MWCNT and SWCNT are examined by field-emission–scanning electron microscopy (FESEM), (JSM 700F, JEOL, Japan). For the preparation of SEM samples, the above-mentioned CNT-NLC mixtures for each kind after sonicating 10 min have been dropped onto the transmission electron microscopy (TEM) grids (100 nm), which have settled on the filtration stage with filter paper. The samples collected over TEM grid have been examined by FESEM.

In order to observe field-dependent behavior of the CNT clusters, an interdigitated electrode with opaque aluminum metal is fabricated on a glass plate and used as the bottom substrate. The top substrate, however, is made of a bare glass plate. Illustration of the test cell driven by an in-plane field is shown in Fig. 2. For providing planar alignment to the negative NLC molecules perpendicular to the applied field direction, the homogeneous alignment layer (SE-6514, Nissan Chemicals) is spin coated on both substrates followed by baking at 200 °C for 1 h and rubbing. It should be noted here that the NLC directors in both NLC-CNT mixtures do not reorient under electric field. The main reason we use nematic LC as the liquid is that it has a high resistivity with 10^{13} Ω cm, so that a relatively high electric field can be tested in the cells without an electrical short. The interdigitated electrodes are 10 μm wide maintaining a 20-μm intraelectrode gap and the final cells having a thickness of 60 μm are constructed. The test cells are filled with the CNT-NLC mixture using a capillary action technique at room temperature. All the textures of the test cells for field-induced cluster stretching behavior are observed by an optical microscope (Nikon DXM1200) while applying a sinusoidal ac field at 60 Hz. All the experimental results shown in the present paper have been performed at room temperature (300 K). The diameter of CNT bundles is determined from 80 samplings in the area of 1 × 1 μm^2.

III. RESULTS AND DISCUSSION

Considering the differences in either kind of CNT structure, the self-assembled MWCNT and SWCNT clusters in NLC medium at initial state have been investigated through SEM, as shown in Fig. 3. Typical SEM images of CNT clusters for comparable size in NLC medium are shown in low (× 10 000) and high (× 50 000) magnification. The lower and higher magnification SEM images of MWCNT clusters are shown in Figs. 3(a) and 3(b) and those of SWCNT clusters are shown in Figs. 3(d) and 3(e). From a comparative macroscopic view it appears that the MWCNT cluster shows larger bend and more compact conformation than the SWCNT cluster. Either kind of cluster appears to comprise nanometric cylindrical CNT bundles. We have investigated diameter distribution of cylindrical CNT bundles for MWCNTs and SWCNTs, as shown in Figs. 3(c) and 3(f). The nanometric cylindrical constituents of MWCNT bundles show a distribution of diameters between 20 and 36 nm and those of SWCNT bundles are between 22 and 40 nm. Considering average outer diameter of individual MWCNTs ∼5 nm, the number of CNTs ranges from 62 to 200, whereas considering the average diameter of individual SWCNTs ∼1.5 nm, the number of CNTs ranges from 253 to 837 in each bundle. However, the bundle-bundle interaction in SWCNT cluster seems to be small, evidenced by the sparse location of SWCNT bundles.

To illustrate the influence of distinct CNT bundle entanglement onto field-induced stretching of their clusters in detail; Fig. 4 shows the representative case studies of SWCNT and MWCNT clusters stretching for comparable lengths in the mentioned cell geometry. The longitudinal length of the SWCNT clusters is 1.8, 2.5, and 4.2 μm. The stretching behavior of SWCNT clusters has been compared with the

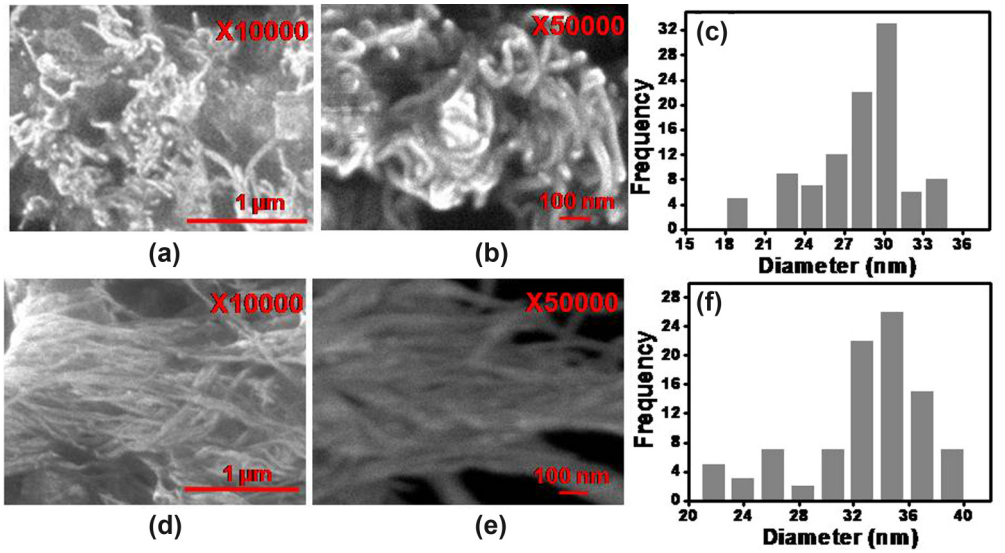

FIG. 3. (Color online) SEM images of initial state of MWCNT (a), (b) and SWCNT (d), (e) cluster in NLC medium. (a), (d) and (b), (e) are SEM images with low magnification (×10 000) and high magnification (×50 000). (c) and (f) are MWCNT and SWCNT diameter distribution according to (b) and (e).

mentioned representative MWCNT cluster lengths of 1.6, 2.3, and 3.8 μm in the zero field state. We define a threshold field (E_{th}) as the field needed to elongate the CNT cluster up to a resolution limit of optical microscopy, i.e., 0.2 μm. The stretching behavior of in-plane electric field-induced CNT clusters is found to initiate at a certain electric field, i.e., E_{th}. This is found to be size dependent and shows an increasing trend as the cluster size increases for the same CNT type. In addition, the optical micrographs show significantly lower threshold field for SWCNT clusters than for MWCNT with similar cluster sizes.

The representative cases of the MWCNT and SWCNT cluster stretching phenomenon shown in Fig. 4 have been quantitatively depicted in Fig. 5. The relative variation in cluster length (Δl) has been plotted as a function of applied in-plane field strength. Here,

$$\Delta l = l_E - l, \tag{1}$$

where l_E and l represent the length of the cluster for applied field strength E state and "zero field" state. It has already been mentioned earlier that the minimum magnitude of Δl is limited by the resolution limit of the optical microscope, i.e., 0.2 μm, and an elongation of the same magnitude has been considered as E_{th} for all CNT clusters in the following discussion. The SWCNT clusters with zero field lengths of 1.8, 2.5, and 4.2 μm are found to start stretching at field strengths of 0.60,

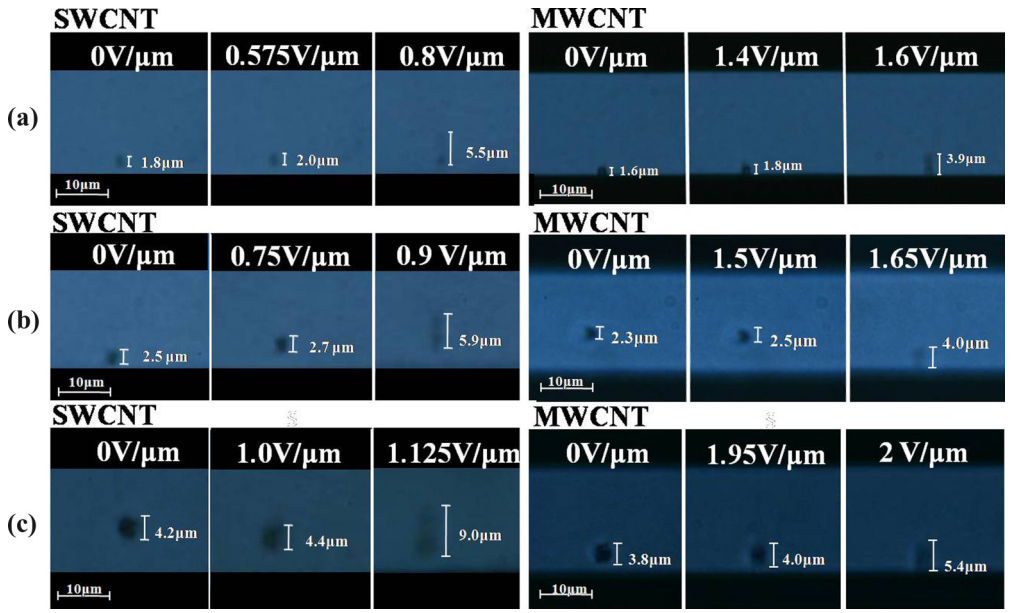

FIG. 4. (Color online) Optical micrographs of representative CNT cluster cases in NLC medium with initial lengths of 1.8 (a), 2.5 (b), and 4.2 μm (c) for SWCNT and 1.6 (a), 2.3 (b), and 3.8 μm (c) for MWCNT depending on electric field.

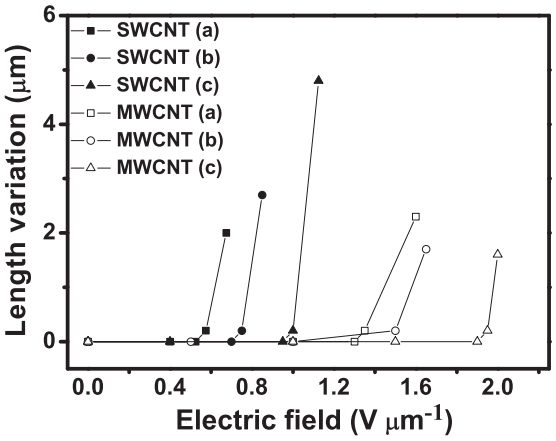

FIG. 5. Length variation of SWCNT and MWCNT clusters as a function of electric field.

0.80, and 1.0 $V_{rms}/\mu m$. However, the MWCNT clusters of zero field lengths of 1.6, 2.3, and 3.8 μm require field strengths of 1.4, 1.5, and 2.0 $V_{rms}/\mu m$ to start stretching. After switching off the applied ac field, the stretched clusters restore to their original state, revealing perfectly elastic behavior. Note that the stretching and restoring process of CNT clusters is perfectly reproducible over hundreds of experimental trials, perfectly agreeing with previously reported CNT cluster stretching results, and also the process is still observed in the isotropic phase of the liquid crystal [17,18].

It is clearly visible from optical micrographs of both SWCNT and MWCNT clusters that for similar experimental conditions and comparable cluster sizes, the E_{th} of stretching is higher in MWCNTs than in SWCNTs. A similar trend has been observed by successive experiments in identical experimental conditions. Such electric field-induced stretching properties of CNT clusters have been reported in previous works [17–20]. The observed stretching phenomenon can be explained by considering applied electric field-induced CNT dipolar reordering [26–28] from random to linear form. After alignment in the field direction, the CNTs in the host medium experience the force $\vec{F}_{elec}$,

$$\vec{F}_{elec} = -q\vec{E} + \vec{p}\cdot\nabla\vec{E} \tag{2}$$

where $\vec{p}$ represents the induced dipole moment and q represents the charge induced on the CNT clusters in the presence of electric field $\vec{E}$. The first term $q\vec{E}$ describes Coulombic interaction between charges of the particles and external field. The additional force term $(\vec{p}\cdot\nabla)\vec{E}$ arises from interaction between the induced dipole of the particle and a spatially inhomogeneous field.

As we know, in the absence of electric field, the CNTs are entangled in the form of bundles due to strong van der Waals interaction. Applied oscillatory electric field induces fast reversing equal and opposite charges in the terminal of tubes. With increasing field, the individual CNTs in bundles are aligned along the field direction to minimize the dipolar energy. Hence, above a certain field, Columbic interaction $q\vec{E}$ overcomes van der Waals forces and CNT clusters start to elongate along the field direction. With further increase of field, individual CNTs will be forced to stretch out from the bundle and CNTs are chained by inter-CNT (dipole-dipole) interactions along the field direction when the Columbic force $q\vec{E}$ further overcomes van der Waals force between CNTs [17,20,27,29].

The above-observed difference in stretching threshold field between SWCNT and MWCNT clusters is influenced by the bending conformation of CNT bundles; inter-CNT bundle interaction will be discussed in detail afterwards. The electric field-induced dipolar character of individual CNTs and suspended clusters formed in NLC medium have been well documented in the literature [17–20]. Consequently, the CNT clusters reorient along the direction of applied electric field as the applied field strength approaches its threshold value, and initiate stretching at the threshold field. The resemblance of prior reports of the bending elastic constant of MWCNTs can be considered as indirect evidence of bending conformation of the present MWCNT cluster, while suspended in NLC matrix [18]. As the stretching behavior of the CNT cluster starts from individual CNT alignment along the field direction, so the stretching threshold field is related to unfolding by straightening the deformed MWCNTs in clusters. The distinct bending CNT deflection in entanglement for each kind obviously affects the threshold stretching. Additionally, it is important to discuss the difference in dipolar character in SWCNT and MWCNT types due to their significant relation with the attractive dipolar interaction of individual CNTs under electric field. The electric field due to a pure dipole at sufficiently large distance $|x–x_0|$ is represented in Eq. (3):

$$\vec{E}_{dip} = \frac{1}{4\pi\varepsilon}\frac{1}{|x-x_0|^3}[3(\vec{p}\cdot\hat{n})\hat{n} - \vec{p}], \tag{3}$$

where $\vec{p}$ is the dipole moment and ε is the permittivity of the medium. However, at limiting small intradipole separation, an additional term needs to be included in order to describe the field strength [29–31],

$$\vec{E}_{dip} = \frac{1}{4\pi\varepsilon}\frac{1}{|x-x_0|^3}[3(\vec{p}\cdot\hat{n})\hat{n} - \vec{p}] - \frac{1}{3\varepsilon}\vec{p}\delta^3(x-x_0). \tag{4}$$

Here, it is necessary to assume the nanotube bundles as a system similar to a cluster of electric dipoles. The assumption has already been examined [18] and applied in this system. The added delta function does not contribute to the field away from the site of the dipole. Its purpose is to yield the required volume integral with the convention that the spherically symmetric (around x_0) volume integral of the first term is zero (from angular integration), the singularity at $x = x_0$ causing an otherwise ambiguous result. Thus the treatment of the above equation can be employed as if we are dealing with idealized point dipoles; the delta function terms carry the essential information about the actually finite distribution of charge.

The average outer MWCNT diameter is ~5 nm and an average length is ~290 nm, which results in an average volume of $\sim 5.7 \times 10^{-24}$ m^3 for an individual MWCNT. Considering the cylindrical conformation of MWCNT clusters as a first approximation, the clusters of our present investigation have lengths lying between 1 and 4 μm and diameters ranging from 2 to 3 μm. Hence, the number ($\sim 10^5$–10^6) of individual MWCNTs is anticipated in each cluster. In contrast, the

average SWCNTs possess an outer diameter of ~1.5 nm and an average length of ~100 nm, which result in an average volume of $\sim 1.8 \times 10^{-25}$ m^3 for an individual SWCNT. Considering the cylindrical conformation of SWCNT clusters as a first approximation, the clusters of our present investigation have lengths lying between 1 and 4.5 μm and diameters ranging from 1 to 3.5 μm. Hence, the number of individual SWCNTs in each cluster ($\sim 10^7$–10^8) is even greater compared with the MWCNT counterpart. As shown in the diameter distribution obtained from SEM investigation [Figs. 3(c) and 3(f)], each cylindrical ropelike SWCNT bundle consists of a significantly larger number of individual CNTs ranging from 253 to 837 compared to apparently similar cylindrical ropelike constituent of MWCNT counterpart ranging from 62 to 200, which reestablishes the above-mentioned statement. In the clustered state either CNT kind occurs in bundle form, where the higher CNT number density in the SWCNT cluster in comparison with the MWCNT counterpart ensures smaller separation between individual SWCNTs. Therefore, the additional delta function introduced as the last term of Eq. (4) becomes more important and relevant while the inter-CNT separation reaches limiting values. Hence, from prior discussion, Eq. (4) establishes its relevance in the case of a SWCNT cluster compared with the MWCNT counterpart, as the SWCNT number density is much higher than MWCNT's in comparable sizes of clusters. The delta function term effectively weakens the individual dipolar field and consequently intradipolar field strength, which causes weaker attractive dipolar interaction between SWCNTs. Thus, sparse separation of SWCNT bundles (Fig. 3) evidences weaker interbundle interaction in contrast with MWCNT bundles. As a result the threshold stretching field appears to be smaller for SWCNT clusters in comparison with the MWCNT counterpart.

To further verify the effect of CNT bundle entanglement and attractive dipolar interaction between adjacent CNT bundles in SWCNT and MWCNT clusters on stretching behavior, electrically induced elastic strains have been examined. We have defined the tensile elasticity modulus of CNT clusters using an analogous parameter of Coulombic Youngs modulus Y. The Y is defined in our case as the ratio of field tensile stress to tensile strain. It can be expressed in the following equation:

$$Y = \frac{E}{\frac{\Delta l}{l}}, \tag{5}$$

where Y represents the tensile elasticity modulus of CNT clusters, and E represents applied electric field strength on the clusters. Since Δl represents the relative variation of the CNT cluster's length and l represents the length of the CNT cluster in the zero field state, $\Delta l/l$ defines the tensile strain over CNT clusters. The highly elastic behavior of the CNT cluster has already been demonstrated by our group in several previous reports [17,18]. Hence it is reasonable to further define the parameter Y for comparison of the elastic behavior of clusters for each kind. The linear relationship between field tensile stress and tensile strain has been exhibited in Fig. 6. The linear curves are showing that extension (strain) is linearly proportional to its tensile stress E and the slope has been defined as tensile elasticity modulus Y, analogous to Young's modulus. The linear nature of the curves self-evidences the highly elastic behavior of the clusters under investigation. Additionally, Y has been quantitatively determined by analyzing elongation of a number of experimentally observed clusters and obtained by the stress-strain curves of SWCNTs and MWCNTs with a given formula. The average value of Y for SWCNT clusters is found to be ~0.12 V_{rms}/μm, which is approximately four times smaller than that of MWCNT clusters (the average value ~0.51 V_{rms}/μm). The difference in parameter Y self-evidences the difference in electrically induced dipolar interaction between SWCNT and MWCNT types in clustered conformation. The larger Y of MWCNT clusters obviously supports comparatively tighter MWCNT bending conformation compared to the SWCNT counterpart, in which the dipolar interaction between MWCNTs is larger than that in SWCNTs. In order to determine the attractive interaction at the threshold field, we further calculate the threshold tensile elasticity modulus with similar sizes for two types, as shown in Fig. 7. The data analyzed at threshold show Y values for SWCNT cluster with zero field lengths of 1.8, 2.5, and 4.2 μm are 5.2, 9.4, and 21.0 V_{rms}/μm. However, Y values for MWCNT clusters with 1.6, 2.3, and 3.8 μm are 10.8, 17.3, and 37.1 V_{rms}/μm. The Y values determined from respective case studies exhibit a higher magnitude for MWCNTs in comparison with the SWCNT

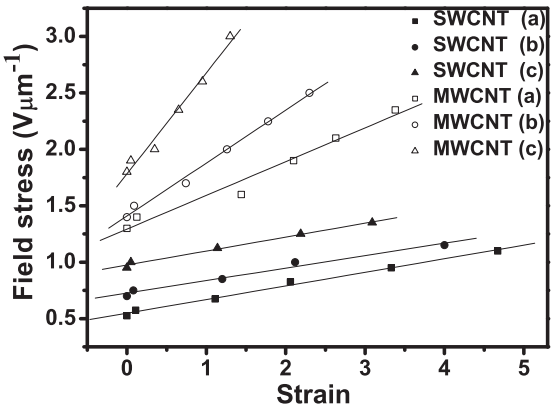

FIG. 6. Electric field stress as a function of strain of stretched CNT clusters. The slope of the fitting curves represents the Coulomb elasticity modulus of each CNT cluster case.

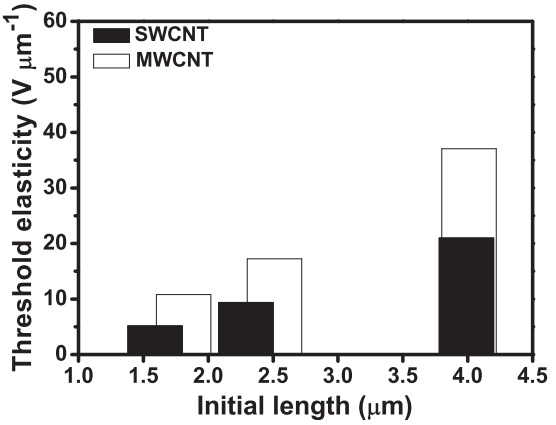

FIG. 7. Comparison of threshold elasticity modulus between SWCNT and MWCNT clusters with comparable lengths.

counterpart at the threshold field, where individual cluster lengths are comparable to one another. The difference in Y value indicates the difference in stiffness in either kind of CNT cluster.

IV. CONCLUSIONS

The structure conformation of SWCNT and MWCNT clusters with similar sizes in NLC medium have been examined by SEM, which shows more entangled bundle conformation of MWCNT than that of SWCNT in clusters. The MWCNT bundles consist of a smaller number of individual CNTs than SWCNT bundles, although the diameters of the bundles are similar to each other. The investigated field-induced stretching threshold field of clusters for each kind is found to be closely connected with distinct entanglement of CNT bundles and is found to be noticeably smaller for SWCNT clusters than for MWCNT clusters for comparable cluster sizes. The behavior has also been explained by different field-induced attractive dipolar interaction between MW and SWCNT clusters. Since the inter-CNT elastic strain at threshold field directly reflects inter-CNT bundle interaction, the obtained smaller magnitude of tensile elasticity modulus for SWCNT clusters evidences smaller attractive interaction between SWCNTs than between MWCNTs.

ACKNOWLEDGMENTS

This work was supported by the National Research Foundation of Korea (NRF) Grant funded by the Korean Government (MSIP) (Grant No. 2014R1A4A1008140) and also by the Institute for Basic Science (IBS).

[1] J. T. Di, D. M. Hu, H. Y. Chen, Z. Z. Yong, M. H. Chen, Z. H. Feng, Y. T. Zhu, and Q. W. Li, ACS Nano **6**, 5457 (2012).
[2] A. D. Franklin and Z. H. Chen, Nat. Nanotechnol. **5**, 858 (2010).
[3] R. Basu and G. S. Iannacchione, Phys. Rev. E **81**, 051705 (2010).
[4] S. J. Tans, M. H. Devoret, H. J. Dai, A. Thess, R. E. Smalley, L. J. Geerligs, and C. Dekker, Nature **386**, 474 (1997).
[5] E. W. Wonder, P. E. Sheehan, and C. M. Lieber, Science **277**, 1971 (1997).
[6] S. Shoji, H. Suzuki, R. P. Zaccaria, Z. Sekkat, and S. Kawata, Phys. Rev. B **77**, 153407 (2008).
[7] S. J. Tans, A. R. M. Verschueren, and C. Dekker, Nature **393**, 49 (1998).
[8] R. H. Baughman, C. X. Cui, A. A. Zakhidov, Z. Iqbal, J. N. Barisci, G. M. Spinks, G. G. Wallace, A. Mzaaoldi, D. D. Ross, A. G. Rinzler, O. Jaschinski, S. Roth, and M. Kertesz, Science **284**, 1340 (1999).
[9] J. Kong, N. R. Franklin, C. W. Zhou, M. G. Capline, S. Peng, K. Cho, and H. Dai, Science **287**, 622 (2000).
[10] Z. C. Wu, Z. H. Chen, X. Du, J. M. Logan, J. Sippel, M. Nikolou, K. Kamaras, J. R. Reynolds, D. B. Tanner, A. F. Hebard, and A. G. Rinzler, Science **305**, 1273 (2004).
[11] S. X. Lu, Y. Liu, N. Shao, and B. Panchapakesan, Nanotechnology **18**, 065501 (2007).
[12] C. S. Li, Y. Liu, X. Z. Huang, and H. R. Jiang, Adv. Funct. Mater. **22**, 5166 (2012).
[13] L. M. Huang, Z. Jia, and S. OBrien, J. Mater. Chem. **17**, 3863 (2007).
[14] W. Q. Fu, L. Liu, K. L. Jiang, Q. Q. Li, and S. S. Fan, Carbon **48**, 1876 (2010).
[15] M. D. Lynch and D. L. Patrick, Nano Lett. **2**, 1197 (2002).
[16] J. Lagerwall, G. Scalia, M. Haluska, U. Dettlaff-Weglikowska, S. Roth, and F. Glesselmann, Adv. Mater. **19**, 359 (2007).
[17] S. J. Jeong, K. A. Park, S. H. Jeong, H. J. Jeong, K. H. An, C. W. Nah, D. Pribat, S. H. Lee, and Y. H. Lee, Nano Lett. **7**, 2178 (2007).
[18] S. S. Bhattacharyya, G. H. Yang, W. W. Tie, Y. H. Lee, and S. H. Lee, Phys. Chem. Chem. Phys. **13**, 20435 (2011).
[19] B. G. Kang, Y. J. Lim, K. U. Jeong, K. Lee, Y. H. Lee, and S. H. Lee, Nanotechnology **21**, 405202 (2010).
[20] P. Sureshkumar, A. K. Srivastava, S. J. Jeong, M. Y. Kim, E. M. Jo, S. H. Lee, and Y. H. Lee, J. Nanosci. Nanotechnol. **9**, 4741 (2009).
[21] K. H. An and Y. H. Lee, NANO **1**, 115 (2006).
[22] R. Saito, G. Dresselhaus, and M. S. Dresselhaus, *Physical Properties of Carbon Nanotubes* (Imperial College Press, London, UK, 1998).
[23] R. S. Ruoff and D. C. Lorents, Carbon **33**, 925 (1995).
[24] K. A. Park, S. M. Lee, S. H. Lee, and Y. H. Lee, J. Phys. Chem. C **111**, 1620 (2007).
[25] S. Y. Jeon, K. A. Park, I. S. Baik, S. J. Jeong, S. H. Jeong, K. H. An, S. H. Lee, and Y. H. Lee, NANO **2**, 41 (2007).
[26] H. W. Seo, C. S. Han, D. G. Choi, K. S. Kim, and Y. H. Lee, Microelectron. Eng. **81**, 83 (2005).
[27] A. K. Srivastava, S. J. Jeong, M. H. Lee, S. H. Lee, S. H. Jeong, and Y. H. Lee, J. Appl. Phys. **102**, 043503 (2007).
[28] W. W. Tie, G. H. Yang, S. S. Bhattacharyya, Y. H. Lee, and S. H. Lee, J. Phys. Chem. C **115**, 21652 (2011).
[29] C. P. Frahm, Am. J. Phys. **51**, 826 (1983).
[30] R. Estrada and R. P. Kanwal, Am. J. Phys. **63**, 278 (1995).
[31] D. J. Griffiths, Am. J. Phys. **50**, 698 (1982).